Volume 1 | Number 1 | Jan 2013 | Pages 1–100

Dalton Transactions

An international journal of inorganic chemistry
www.rsc.org/dalton

ROYAL SOCIETY OF CHEMISTRY

ROYAL SOCIETY OF CHEMISTRY

www.rsc.org/dalton

ARTICLE TYPE

Dimensionality variations in new zirconium iodates: hydrothermal syntheses, structure determinations, and characterizations of BaZr(IO$_3$)$_6$ and K$_2$Zr(IO$_3$)$_6$

Hyun Sun Ahn, Dong Woo Lee, and Kang Min Ok*

Two new quaternary zirconium iodates, BaZr(IO$_3$)$_6$ and K$_2$Zr(IO$_3$)$_6$ have been synthesized through hydrothermal reactions by using BaCO$_3$ (or K$_2$CO$_3$), ZrO$_2$, and HIO$_3$ as reagents. Single crystal 10 and powder X-ray diffraction were used to determine crystal structures of the compounds. BaZr(IO$_3$)$_6$ exhibits infinite bands that are composed of ZrO$_7$ pentagonal bipyramids and IO$_3$ trigonal pyramids, in which Ba^{2+} cations are sandwiched by the bands. K$_2$Zr(IO$_3$)$_6$ exhibits a molecular structure that is composed of ZrO$_6$ octahedra and IO$_3$ groups. The dimensionality variations seem to be attributable to the flexible coordination numbers of Zr^{4+} cations with large 15 ionic radii as well as the number of counter cations. Both of the materials are thermally stable up to approximately 440–450 °C and then decompose to the corresponding metal zirconium oxides above the temperatures. The band gaps for BaZr(IO$_3$)$_6$ and K$_2$Zr(IO$_3$)$_6$ are calculated to be 3.1 and 3.0 eV, respectively, using the (K/S)-versus-E plots obtained from the UV-vis diffuse reflectance spectra. Infrared spectra and local dipole moment calculations are also presented.

Introduction

20 Owing to their technologically very important characteristics such as piezoelectricity, second-harmonic generation (SHG), ferroelectricity, and pyroelectricity, macroscopic noncentrosymmetric (NCS) materials have been continuously 25 explored.[1] Thus, the development of advanced new NCS materials with asymmetric structural building units is currently of great interest. With oxide materials exhibiting extended structures, the NCS compounds are normally observed from two families of cations, i.e., octahedrally 30 coordinated d^0 transition metal cations (Ti^{4+}, V^{5+}, Nb^{5+}, Mo^{6+}, W^{6+}, etc.) and cations with stereoactive lone pairs (Pb^{2+}, Sb^{3+}, Se^{4+}, Te^{4+}, I^{5+}, etc.). The asymmetric coordination environments for both classes of cations are considered to be the result of second-order Jahn-Teller (SOJT) effects.[2] The 35 SOJT effects for the d^0 transition metal cations in octahedral coordination environments generally occur when the empty metal d-orbitals mix with the filled ligand p-orbitals. By doing so, the octahedral distortions normally occur along one of three directions: toward a corner (local C$_4$ direction), toward a 40 face (local C$_3$ direction), or toward an edge (local C$_2$ direction).[3] On the other hand, the strong mutual interaction of the s- and p-orbitals of cation with the p-orbitals of anion is critical for cationic distortion for the lone pair cations.[4] A very successful class of NCS materials synthesized by 45 combining both families of SOJT cations is d^0 transition metal iodates.[5-8] Furthermore, the overall centricities of the metal iodates compounds have been successfully controlled by the introduced cations. For example, a series of alkali-metal titanium iodates with the stoichiometry A$_2$Ti(IO$_3$)$_6$ (A = Li, 50 Na, K, Rb, Cs) have been reported, in which all stoichiometrically similar compounds exhibit molecular

structures composed of a TiO$_6$ octahedron connected to six IO$_3$ polyhedra.[8] Interestingly, the size of alkali metal cation and coordination requirement played important roles to 55 control the macroscopic polarity of the series of compounds. Similar influence of the alkali metal cations on the architecture of crystal structures have been observed from a series of alkali metal molybdenyl iodates as well.[5] Herein we report hydrothermal synthesis, structure determination, and 60 characterization of two new quaternary zirconium iodates, BaZr(IO$_3$)$_6$ and K$_2$Zr(IO$_3$)$_6$. We will describe in this paper how the dimensionality variations of zirconium iodates compounds occur by the effect of d^0 transition metal cation size and number of counter cations.

65 ## Experimental

Reagents

BaCO$_3$ (Daejung, 99%), K$_2$CO$_3$ (Jin Chemical, 99.5%), ZrO$_2$ (Kanto, 99%), Zr(NO$_3$)$_4$ (Acros, 99%), and HIO$_3$ (Alfa Aesar, 99%) were used as received.

70

Synthesis

For BaZr(IO$_3$)$_6$, 0.197 g (1.00 × 10^{-3} mol) of BaCO$_3$, 0.123 g (1.00 × 10^{-3} mol) of ZrO$_2$, 1.055 g (6.00 × 10^{-3} mol) of HIO$_3$, and 5 mL of deionized water were combined. With K$_2$Zr(IO$_3$)$_6$, 75 0.414 g (3.00 × 10^{-3} mol) of K$_2$CO$_3$, 0.339 g (1.00 × 10^{-3} mol) of Zr(NO$_3$)$_4$, 1.055 g (6.00 × 10^{-3} mol) of HIO$_3$, and 5 mL of deionized water were combined. Each reaction mixture was transferred to 23 mL of Teflon-lined stainless steel autoclaves. The autoclaves were tightly sealed and heated to 230 °C for 4 80 days, and cooled to room temperature at a rate of 6 °C h^{-1}. After cooling, the reactors were opened and the products were

filtered and washed with distilled water. While colorless block crystals and powdered samples of $BaZr(IO_3)_6$ were obtained in 77% yield based on $BaCO_3$, polycrystalline phase was isolated in 89% yield based on K_2CO_3 for $K_2Zr(IO_3)_6$. Powder X-ray
[5] diffraction patterns on the bulk samples revealed that the synthesized materials were pure and in very good agreement with the generated patterns from the single-crystal data (see the ESI).

Single-crystal X-ray diffraction
[10]

The crystal structure of $BaZr(IO_3)_6$ was determined by a standard crystallographic method. A colorless block crystal $(0.027 \times 0.033 \times 0.043$ mm^3) of $BaZr(IO_3)_6$ was used for single crystal structure analysis. Diffraction data were
[15] collected at room temperature using a Bruker SMART BREEZE diffractometer equipped with a CCD area detector using graphite monochromated Mo Kα radiation. A narrow-frame method was used with an exposure time of 10 s/frame, and scan widths of 0.30° in omega to collect a hemisphere of
[20] data. The first 50 frames were remeasured at the end of the data collection to monitor instrument and crystal stability. The maximum correction applied to the intensities was < 1%. The data were integrated using the SAINT program,[9] with the intensities corrected for polarization, Lorentz factor, air
[25] absorption, and absorption attributable to the variation in the path length through the detector faceplate. The data were solved with SHELXS-97[10] and refined using SHELXL-97.[11] All calculations were performed using the WinGX-98 crystallographic software package.[12] Crystallographic data
[30] and selected bond lengths for $BaZr(IO_3)_6$ are summarized in Tables 1 and 2, respectively.

Powder X-ray diffraction

The powder XRD data were collected on a Bruker D8-
[35] Advance diffractometer using Cu Kα radiation at room temperature with 40 kV and 40 mA. The diffraction pattern for $K_2Zr(IO_3)_6$ was analyzed using the Rietveld method with the GSAS program.[13] The structural refinement of the material was performed in the space group R-3 (No. 148) with a
[40] starting model of the crystal data of $Rb_2Zr(IO_3)_6$.[14] Crystallographic data and selected bond distances for $K_2Zr(IO_3)_6$ are summarized in Tables 1 and 2, respectively. Also, atomic positions and isotropic displacement parameters for the material have been deposited in the ESI.
[45]

Infrared spectroscopy

Infrared spectra for $BaZr(IO_3)_6$ and $K_2Zr(IO_3)_6$ were recorded on a Varian 1000 FT-IR spectrometer in the 400–4000 cm^{-1} range, with the samples embedded in KBr matrixes.
[50]

UV-vis diffuse reflectance spectroscopy

UV-visible diffuse reflectance data were obtained on a Varian Cary 500 scan UV-vis-NIR spectrophotometer at the Korea Photonics Technology Institute over the spectral range
[55] 200–2500 nm at room temperature. Reflectance spectra were transformed into the absorbance using the Kubelka-Munk function.[15]

Table 1 Crystallographic data for $BaZr(IO_3)_6$ and $K_2Zr(IO_3)_6$

Empirical formula	$BaZrI_6O_{18}$	$K_2ZrI_6O_{18}$
Formula weight	1277.95	1218.82
Crystal system	Triclinic	Trigonal
Space group	P-1 (No. 2)	R-3 (No. 148)
a/Å	7.7497(3)	11.4401(8)
b/Å	7.7663(3)	11.4401(8)
c/Å	14.7514(6)	11.4437(10)
α/°	91.129(3)	90
β/°	102.966(3)	90
γ/°	90.850(3)	120
V / $Å^3$	864.86(6)	1297.04(19)
Z	2	3
T / K	298.0(2)	298.0(2)
λ / Å	0.71073	1.5406
$R(F)^a$ or $R_p{}^b$	0.0421	0.0682
$R_w(F_o{}^2)^c$ or $R_{wp}{}^d$	0.0473	0.0874

$^aR(F)=\Sigma||F_o| - |F_c|| / \Sigma |F_o|.$ $^bR_p = \Sigma |I_o - I_c| / \Sigma I_o.$

[60] $^cR_w(F^2) = [\Sigma w(F_o{}^2 - F_c{}^2)^2 / \Sigma w(F_o{}^2)^2]^{1/2}.$ $^dR_{wp} = [\Sigma w |I_o - I_c|^2 / \Sigma w I_o{}^2]^{1/2}.$

Table 2 Selected bond distances (Å) for $BaZr(IO_3)_6$ and $K_2Zr(IO_3)_6$

$BaZr(IO_3)_6$			
Zr(1)–O(2)	2.163(7)	I(3)–O(7)	1.820(7)
Zr(1)–O(6)	2.125(8)	I(3)–O(8)	1.851(7)
Zr(1)–O(8)	2.197(7)	I(3)–O(9)	1.803(7)
Zr(1)–O(12)	2.045(7)	I(4)–O(10)	1.803(7)
Zr(1)–O(14)	2.218(7)	I(4)–O(11)	1.799(7)
Zr(1)–O(16)	2.139(7)	I(4)–O(12)	1.817(7)
Zr(1)–O(18)	2.045(7)	I(5)–O(13)	1.791(8)
I(1)–O(1)	1.789(7)	I(5)–O(14)	1.839(7)
I(1)–O(2)	1.834(7)	I(5)–O(15)	1.798(8)
I(1)–O(3)	1.796(8)	I(6)–O(3)	2.395(7)
I(2)–O(4)	1.777(8)	I(6)–O(16)	1.848(7)
I(2)–O(5)	1.779(8)	I(6)–O(17)	1.758(8)
I(2)–O(6)	1.853(7)	I(6)–O(18)	1.817(7)
$K_2Zr(IO_3)_6$			
Zr(1)–O(1) × 6	2.092(12)	I(1)–O(2)	1.765(11)
I(1)–O(1)	1.818(13)	I(1)–O(3)	1.798(10)

[65] ### Thermogravimetric analysis (TGA)

Thermogravimetric analysis was performed on a Setaram LABSYS TG-DTA Thermogravimetric Analyzer. The polycrystalline samples of $BaZr(IO_3)_6$ and $K_2Zr(IO_3)_6$ were contained within alumina crucibles and heated from room
[70] temperature to 1000 °C at a rate of 10 °C min^{-1} under flowing argon.

Scanning electron microscope/energy dispersive analysis by X-ray (SEM/EDAX)

[75] SEM/EDAX has been carried out using a Hitachi S-3400N and a Horiba Energy EX-250 instrument. EDAX for $BaZr(IO_3)_6$ and $K_2Zr(IO_3)_6$ reveals Ba:Zr:I and K:Zr:I ratios of 0.8:1.0:5.7 and 1.7:1.0:5.6, respectively.

Results and discussions

Crystal structure description of BaZr(IO$_3$)$_6$

BaZr(IO$_3$)$_6$ is a new quaternary alkaline earth metal zirconium iodate that crystallizes in the triclinic space group, *P*-1 (No. 2). The framework of BaZr(IO$_3$)$_6$ consists of ZrO$_7$ and IO$_3$ polyhedra with Zr–O–I and I–O–I bonds. The unique d^0 transition metal cation, Zr^{4+} is in a slightly distorted pentagonal bipyramidal coordination environment with five equatorial and two axial oxygen atoms (see Fig. 1). While the Zr–O bonds in the axial positions [Zr(1)–O(12) and Zr(1)–O(18)] at the ZrO$_7$ pentagonal bipyramid reveal relatively shorter Zr–O lengths of 2.045(7) Å, those in the equatorial positions exhibit slightly longer Zr–O distances ranging from 2.125(8) to 2.218(7) Å. The O–Zr–O bond angles range from 69.4(3) to 170.1(3)°. Within an asymmetric unit, six unique I^{5+} cations exist under unsymmetrical coordination environments attributable to the stereoactive lone pairs. Most I^{5+} cations are connected by three oxygen atoms in trigonal pyramidal environment with I–O bond distances ranging 1.777(8)–1.853(7) Å; however, the I(6)$^{5+}$ cation reveals a long I–O interaction [2.395(7) Å] as well. It has been suggested that the bond valence calculations may help to justify the choices between chemical bonds and interactions in the case of structures with intermediate interatomic distances.[16] The environment of I^{5+} in iodate groups is often formed by three strong bonds corresponding to an AX$_3$E conformation.[17] In addition, the environment of I^{5+} is filled up by three weak interactions with mean distances ranging from 2.40 to 3.10 Å, which are arranged around the lone pair direction. Similarly, three very long I⋯O contacts ranging from 2.556(8) to 3.294(9) Å are observed toward lone pairs from all six iodates in BaZr(IO$_3$)$_6$. Examples of the tetraoxoiodate(V), [IO$_4$]$^{3-}$, anion have been observed from Ag$_4$(UO$_2$)$_4$(IO$_3$)$_2$(IO$_4$)$_2$O$_2$ and Ba[(MoO$_2$)$_6$(IO$_4$)$_2$O$_4$]·H$_2$O,[18] in which four oxygen atoms in IO$_4$ groups bent away from a tetrahedral coordination into a seesaw geometry. However, as we mentioned earlier, I(6)$^{5+}$ in BaZr(IO$_3$)$_6$ possesses three intermediate and one long I–O bonds. Similar coordination environments with variable geometries and bond distances have been observed from tellurites with lone pairs.[19] The Ba^{2+} cations interact with ten oxygen atoms with Ba–O contact distances ranging from 2.713(7) to 3.112(6) Å. The distorted ZrO$_7$ pentagonal bipyramids are connected to five IO$_3$ groups by sharing their corners through O(2), O(6), O(8), O(12), and O(14) and form a ZrO$_2$(IO$_3$)$_5$ unit (see Fig. 2a). Then the ZrO$_2$(IO$_3$)$_5$ units are linked by IO$_3$ groups through O(16) and O(18), which results in a Zr$_2$(IO$_3$)$_{12}$ group (see Fig. 2b). Further, as seen in Fig. 2c, each Zr$_2$(IO$_3$)$_{12}$ group shares O(3) in I(6)O$_3$ polyhedra and forms an infinite bands along [010] direction. Within the infinite band, four-membered rings (4MRs) and six-membered rings (6MRs) are observed. In connectivity terms, the framework structure of BaZr(IO$_3$)$_6$ can be described as an anionic band of {[ZrO$_{7/2}$]$^{-3}$ [IO$_{2/2}$O$_{1/1}$]$^{+1}$ 6[IO$_{1/2}$O$_{2/1}$]^0}$^{-2}$. Ba^{2+} cations sandwiched in between the anionic bands retain the charge balance (see Fig. 2d). Bond valence sum calculations[20] for the Ba^{2+}, Zr^{4+}, and I^{5+} result in values of 2.04, 4.05, and 4.95–5.18, respectively.
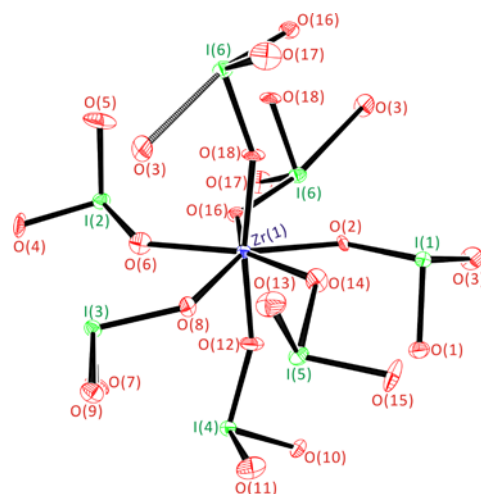
Fig. 1 ORTEP (50% probability ellipsoids) drawing of BaZr(IO$_3$)$_6$ showing ZrO$_7$, and IO$_3$ polyhedra. Note that the I(6)$^{5+}$ cation contains a long I(6)–O(3) interaction.
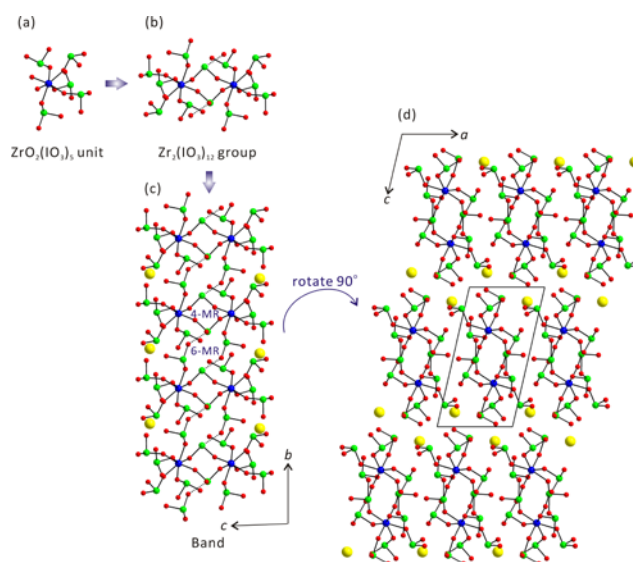

Fig. 2 Ball-and-stick representations of (a) a ZrO$_2$(IO$_3$)$_5$ unit obtained by the connection of five IO$_3$ groups to ZrO$_7$ pentagonal bipyramids, (b) a Zr$_2$(IO$_3$)$_{12}$ group constructed by the linking of I(6)O$_3$ groups to the two ZrO$_2$(IO$_3$)$_5$ units, and completed bands for BaZr(IO$_3$)$_6$ in the (c) *bc*-plane and (d) *ac*-plane (blue, Zr; green, I; yellow, Ba; red, O).

Crystal structure description of K$_2$Zr(IO$_3$)$_6$

The newly synthesized potassium zirconium iodate, K$_2$Zr(IO$_3$)$_6$ is structurally similar to several quaternary transition metal iodates.[14, 21] Since the pure polycrystalline phase of K$_2$Zr(IO$_3$)$_6$ was obtained, the Rietveld method using the powder X-ray diffraction data was employed for the structural analysis. As can be seen from the experimental, calculated, and difference diffraction plots in Fig. 3, the structure of K$_2$Zr(IO$_3$)$_6$ was successfully refined in the trigonal space group *R*-3 (No. 148). K$_2$Zr(IO$_3$)$_6$ is a zero-dimensional molecular compound containing ZrO$_6$ octahedra and asymmetric IO$_3$ groups (see Fig. 4). A unique Zr^{4+} cation is bonded to six oxygen atoms in an octahedral coordination environment with an identical Zr–O bond length of 2.092(12) Å. Also a unique I^{5+} cation is in a trigonal pyramidal

coordination environment with three oxygen atoms with I–O bond lengths ranging over 1.765(11)–1.818(13) Å. The K^+ cations are in ninefold coordination environment with K–O contact distances in the range over 2.957(14)–2.996(12) Å. In connectivity terms, the structure of $K_2Zr(IO_3)_6$ can be written as a huge anion of $\{[ZrO_{6/2}]^{2-} \ 6[IO_{1/2}O_{2/1}]^0\}^{2-}$, with charge balance retained by the K^+ cations. Bond valence sum calculations[20] result in values of 0.95, 3.79, and 4.63 for K^+, Zr^{4+}, and I^{5+}, respectively.

Dimensionality variations

Although the reported zirconium iodates compounds, $BaZr(IO_3)_6$ and $K_2Zr(IO_3)_6$ are stoichiometrically similar, $BaZr(IO_3)_6$ shows a structure with infinite bands yet $K_2Zr(IO_3)_6$ exhibits a molecular geometry. In fact, most of the reported alkali- (or alkaline earth) titanium (or zirconium) iodates with similar stoichiometry reveal zero-dimensional structures.[7, 8, 14, 21] One can easily find that the dimensionality variations are attributable to the flexible coordination numbers of Zr^{4+} cations with large ionic radii as well as the number of counter cations. For example, the ionic radius of seven-coordinate Zr^{4+} in $BaZr(IO_3)_6$ is 0.78 Å, whereas that of six-coordinate Ti^{4+} in $BaTi(IO_3)_6$[21] is 0.605 Å.[22] In other words, the larger Zr^{4+} cation can adopt more iodate ligands around the coordination environment, which enables to form wide bands in $BaZr(IO_3)_6$. However, the smaller coordination environment of Ti^{4+} cation in $BaTi(IO_3)_6$ can adopt only six iodates ligands, in which the lone pairs on IO_3 polyhedra located *trans* to each other are oriented in opposite directions and a molecular structure is obtained. Although the ionic radius of Zr^{4+} in $K_2Zr(IO_3)_6$ is large enough, however, the number of counter cations, i.e., K^+ ions is doubled than that of $BaZr(IO_3)_6$. Thus, the crowded environments of zirconium iodates separated by many K^+ cations have $K_2Zr(IO_3)_6$ to crystallize in a zero-dimensional compound.
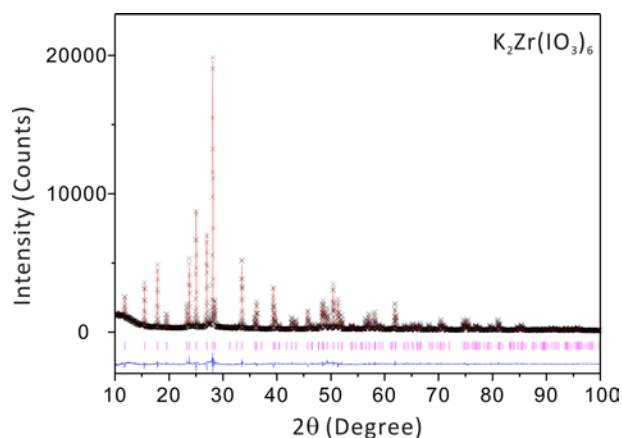

Fig. 3 Final Rietveld plot of $K_2Zr(IO_3)_6$. The calculated pattern (red solid line) is compared with observed data (×). The positions of reflections are indicated by the magenta vertical bars. The difference between the observed and calculated profiles is shown at the bottom (blue solid line).
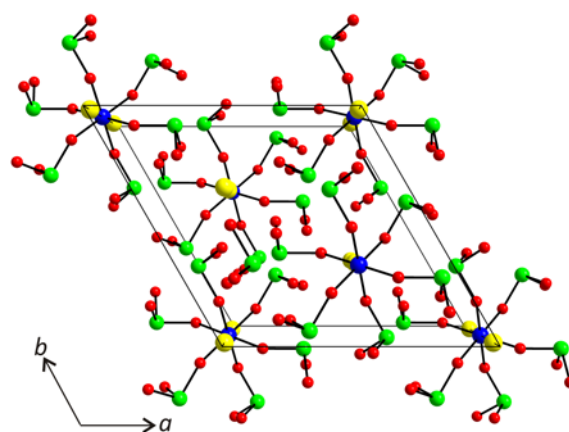

Fig. 4 Ball-and-stick representations of $K_2Zr(IO_3)_6$ in the *ab*-plane (blue, Zr; green, I; yellow, K; red, O).

Infrared spectroscopy

As seen in Fig. 5, Zr–O and I–O vibrations are observed in the infrared spectra of $BaZr(IO_3)_6$ and $K_2Zr(IO_3)_6$. The Zr–O vibrations are found at ca. 696–840 cm^{-1}. Also, the I–O vibrations are occurring at about 409–450 cm^{-1}. The assignments are well agreed with those previously reported materials.[21, 23]
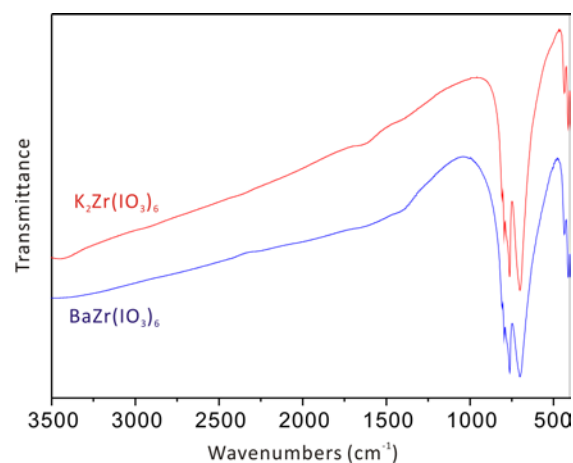

Fig. 5 Infrared spectra of $BaZr(IO_3)_6$ and $K_2Zr(IO_3)_6$.

UV-vis diffuse reflectance spectroscopy

UV-vis diffuse reflectance spectral data for $BaZr(IO_3)_6$ and $K_2Zr(IO_3)_6$ have been collected. Absorption (*K/S*) data were calculated from the Kubelka-Munk function:[15]

$$F(R) = \frac{(1-R)^2}{2R} = \frac{K}{S}$$

in which *R* is the reflectance, *S* the scattering, and *K* the absorption. In the (*K/S*)-versus-*E* plots, extrapolating the linear part of the ascending curve to zero yielded the onset of absorption at 3.1 and 3.0 eV for $BaZr(IO_3)_6$ and $K_2Zr(IO_3)_6$, respectively (see Fig. 6). The band gaps for the reported materials may be attributed to the interaction of I–O and Zr–O bonds, as well as the distortions arising from IO_3 polyhedra.

The onsets of absorption values for the reported compounds are in good agreement with the previous studies of d^0 transition metal iodates materials.[5, 8]
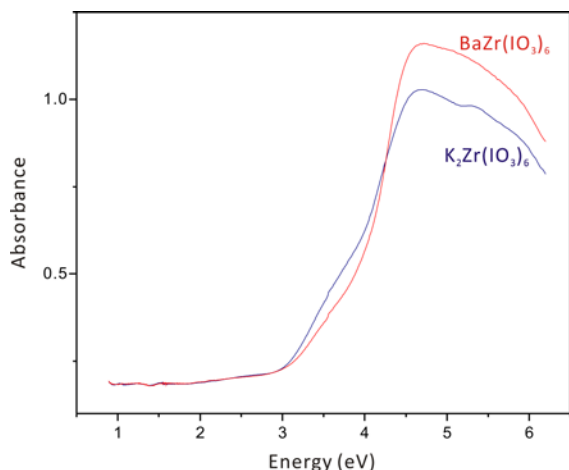

Fig. 6 UV-vis diffuse reflectance spectra of $BaZr(IO_3)_6$ and $K_2Zr(IO_3)_6$ revealing the absorption edges at 3.1 and 3.0 eV, respectively.

Themogravimetric analysis

Thermogravimetric analysis was used to examine the thermal properties of $BaZr(IO_3)_6$ (see Fig. 7). As seen in Fig. 7, both $BaZr(IO_3)_6$ and $K_2Zr(IO_3)_6$ are not stable at higher temperatures. $BaZr(IO_3)_6$ and $K_2Zr(IO_3)_6$ thermally disproportionate at 450 and 440 °C, respectively. The materials completely decompose to $BaZrO_3$ (PDF-# 74-1299) and K_2ZrO_3 (PDF-# 72-0824) by 1000 °C, which were confirmed by the powder XRD. The XRD patterns for the calcined products have been included in the ESI.
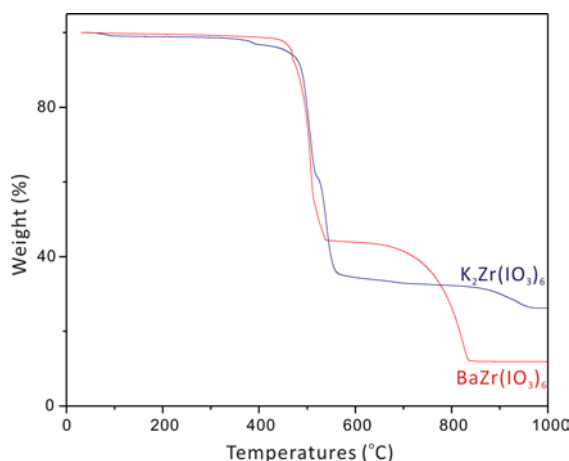

Fig. 7 Thermogravimetric analyses diagrams of $BaZr(IO_3)_6$ and $K_2Zr(IO_3)_6$.

Dipole moment calculations

Although the reported compounds crystallize in macroscopic centrosymmetric space groups, both materials contain asymmetric polyhedra, i.e., IO_3 groups attributable to the stereoactive lone pairs. Thus, it would be interesting to quantify the asymmetric environment of the constituent polyhedra through local dipole moment calculations using the method described earlier.[24] We found that the local dipole moments for IO_3 polyhedra in $BaZr(IO_3)_6$ and $K_2Zr(IO_3)_6$ are calculated to be about 12.5–15.6 D (Debyes), which are similar values to those of reported iodates materials.[21, 25] The local dipole moments for the IO_3 groups are summarized in Table 3.

Table 3 Calculation of dipole moments for IO_3 and IO_4 polyhedra. D = Debyes.

Compound	Species	Dipole moment (D)
$BaZr(IO_3)_6$	$I(1)O_3$	15.6
	$I(2)O_3$	14.9
	$I(3)O_3$	13.6
	$I(4)O_3$	14.5
	$I(5)O_3$	14.6
	$I(6)O_3$	12.5
$K_2Zr(IO_3)_6$	$I(1)O_3$	13.2

Conclusions

Pure phases of two new quaternary metal zirconium iodates compounds, i.e., $BaZr(IO_3)_6$ and $K_2Zr(IO_3)_6$ have been successfully synthesized through hydrothermal reactions in high yields. Crystal structure analyses reveal that $BaZr(IO_3)_6$ reveals an infinite band structure that is composed of ZrO_7 and IO_3 polyhedra, whereas $K_2Zr(IO_3)_6$ exhibits a molecular structure with ZrO_6 and IO_3 polyhedra. The size of coordination environment of transition metal cations and the number of counter cations seem to play important roles to determine the dimensions of stoichiometrically similar transition metal iodates compounds. Detailed spectroscopic characterizations, elemental analyses, thermal analyses, and dipole moment calculations have been also presented on the reported materials.

Acknowledgements

Notes and references

*Department of Chemistry, Chung-Ang University, Seoul, 156-756, Republic of Korea. Fax: 82 2 825 4736; Tel: 82 2 820 5197; E-mail: kmok@cau.ac.kr
†Electronic Supplementary Information (ESI) available: X-ray crystallographic file in CIF format, calculated and observed X-ray diffraction patterns, and XRD patterns for the calcined products for $BaZr(IO_3)_6$ and $K_2Zr(IO_3)_6$. See DOI: 10.1039/b000000x/

1. (a) J. F. Nye, *Physical Properties of Crystals*, Oxford Univ. Press, Oxford, 1957; (b) F. Jona and G. Shirane, *Ferroelectric Crystals*,

Pergamon Press, Oxford, 1962; (c) W. G. Cady, *Piezoelectricity; an Introduction to the Theory and Applications of Electromechanical Phenomena in Crystals*, Dover, New York, 1964; (d) S. B. Lang, *Sourcebook of Pyroelectricity*, Gordon & Breach Science, London, 1974;
5 (e) K. M. Ok, E. O. Chi and P. S. Halasyamani, *Chem. Soc. Rev.*, 2006, **35**, 710.

2. (a) U. Opik and M. H. L. Pryce, *Proc. R. Soc. London*, 1957, **A238**, 425; (b) R. F. W. Bader, *Can. J. Chem.*, 1962, **40**, 1164; (c) R. G. Pearson, *J. Am. Chem. Soc.*, 1969, **91**, 4947; (d) R. G. Pearson, *J. Mol. Struct.:*
10 *THEOCHEM*, 1983, **103**, 25; (e) R. A. Wheeler, M.-H. Whangbo, T. Hughbanks, R. Hoffmann, J. K. Burdett and T. A. Albright, *J. Am. Chem. Soc.*, 1986, **108**, 2222; (f) M. Kunz and I. D. Brown, *J. Solid State Chem.*, 1995, **115**, 395.

3. (a) P. S. Halasyamani and K. R. Poeppelmeier, *Chem. Mater.*, 1998, **10**,
15 2753; (b) P. S. Halasyamani, *Chem. Mater.*, 2004, **16**, 3586.

4. (a) I. Lefebvre, M. Lannoo, G. Allan, A. Ibanez, J. Fourcade and J. C. Jumas, *Phys. Rev. Lett.*, 1987, **59**, 2471; (b) I. Lefebvre, M. A. Szymanski, J. Olivier-Fourcade and J. C. Jumas, *Phys. Rev. B.*, 1998, **58**, 1896; (c) G. W. Watson and S. C. Parker, *J. Phys. Chem. B.*, 1999, **103**, 1258; (d) G.
20 W. Watson, S. C. Parker and G. Kresse, *Phys. Rev. B*, 1999, **59**, 8481; (e) R. Seshadri and N. A. Hill, *Chem. Mater.*, 2001, **13**, 2892; (f) U. V. Waghmare, N. A. Spaldin, H. C. Kandpal and R. Seshadri, *Phys. Rev. B*, 2003, **67**, 125111; (g) A. Walsh, D. J. Payne, R. G. Egdell and G. W. Watson, *Chem. Soc. Rev.*, 2011, **40**, 4455.

25 5. R. E. Sykora, K. M. Ok, P. S. Halasyamani and T. E. Albrecht-Schmitt, *J. Am .Chem. Soc.*, 2002, **124**, 1951.

6. (a) R. E. Sykora, K. M. Ok, P. S. Halasyamani, D. M. Wells and T. E. Albrecht-Schmitt, *Chem. Mater.*, 2002, **14**, 2741; (b) T. C. Shehee, R. E. Sykora, K. M. Ok, P. S. Halasyamani and T. E. Albrecht Schmitt, *Inorg.*
30 *Chem.*, 2003, **42**, 457; (c) R. E. Sykora and T. E. Albrecht Schmitt, *Inorg. Chem.*, 2003, **42**, 2179; (d) C.-F. Sun, C.-L. Hu, X. Xu, J.-B. Ling, T. Hu, F. Kong, X.-F. Long and J.-G. Mao, *J. Am. Chem. Soc.*, 2009, **131**, 9486; (e) C. Sun, T. Hu, X. Xu and J. G. Mao, *Dalton Trans.*, 2010, **39**, 7960; (f) B. Yang, C. Hu, X. Xu, C. Sun, H. Zhang Jian and J. G. Mao, *Chem.*
35 *Mater.*, 2010, **22**, 1545; (g) C.-F. Sun, C.-L. Hu, X. Xu, B.-P. Yang and J.-G. Mao, *J. Am. Chem. Soc.*, 2011, **133**, 5561; (h) C. Huang, C.-L. Hu, X. Xu, B.-P. Yang and J.-G. Mao, *Dalton Trans.*, 2013, **42**, 7051; (i) B.-P. Yang, C.-L. Hu, X. Xu, C. Huang and J.-G. Mao, *Inorg. Chem.*, 2013, **52**, 5378.

40 7. H. Y. Chang, S.-H. Kim, P. S. Halasyamani and K. M. Ok, *J. Am. Chem. Soc.*, 2009, **131**, 2426.

8. H.-Y. Chang, S.-H. Kim, K. M. Ok and P. S. Halasyamani, *J. Am. Chem. Soc.*, 2009, **131**, 6865.

9. *SAINT, Program for Area Detector Absorption Correction*; *version*
45 *4.05;* Siemens Analytical X-ray Instruments: Madison, WI, USA, 1995.

10. G. M. Sheldrick, *SHELXS-97 - A program for automatic solution of crystal structures*; University of Goettingen, Goettingen, Germany, 1997.

11. G. M. Sheldrick, *SHELXL-97 - A program for crystal structure refinement*; University of Goettingen: Goettingen, Germany, 1997.

50 12. L. J. Farrugia, *J. Appl. Crystallogr.*, 1999, **32**, 837.

13. A. C. Larson and R. B. von Dreele, *General Structural Analysis System (GSAS)*, Los Alamos National Laboratory, Los Alamos, NM, 1987.

14. T. C. Shehee, S. F. Pehler and T. E. Albrecht-Schmitt, *J. Alloys Compds.*, 2005, **388**, 225.

55 15. (a) P. Kubelka and F. Munk, *Z. Tech. Phys.*, 1931, **12**, 593; (b) J. Tauc, *Mater. Res. Bull.*, 1970, **5**, 721.

16. I. Gautier-Luneau, Y. Suffren, H. Jamet and J. Pilmé, *Z. Anorg. Allg. Chem.*, 2010, **636**, 1368.

17. I. D. Brown, *J. Solid State Chem.*, 1974, **11**, 214.

60 18. (a) A. C. Bean, C. F. Campana, O. Kwon and T. E. Abrecht-Schmitt, *J. Am. Chem. Soc.*, 2001, **123**, 8806; (b) R. E. Sykora, D. M. Wells and T. E. Albrecht-Schmitt, *Inorg. Chem.*, 2002, **41**, 2697.

19. (a) K. M. Ok and P. S. Halasyamani, *Chem. Mater.*, 2001, **13**, 4278; (b) K. M. Ok, J. Orzechowski and P. S. Halasyamani, *Inorg. Chem.*, 2004,
65 **43**, 964; (c) D. W. Lee, S.-J. Oh, P. S. Halasyamani and K. M. Ok, *Inorg. Chem.*, 2011, **50**, 4473; (d) Y. H. Kim, D. W. Lee and K. M. Ok, *Inorg. Chem.*, 2013, **52**, 11450; (e) Y. H. Kim, D. W. Lee and K. M. Ok, *Inorg. Chem.*, 2014, **53**, 1250.

20. (a) I. D. Brown and D. Altermatt, *Acta Crystallogr.*, 1985, **B41**, 244;
70 (b) N. E. Brese and M. O'Keeffe, *Acta Crystallogr.*, 1991, **B47**, 192.

21. (a) F. Schellhaas, H. Hartl and R. Frydrych, *Acta Crystallogr.*, 1972, **B28**, 2834; (b) K. M. Ok and P. S. Halasyamani, *Inorg. Chem.*, 2005, **44**, 2263.

22. R. D. Shannon, *Acta Crystallogr.*, 1976, **A32**, 751.

75 23. E. S. Elshazly and O. A. A. Abdelal, *Int. J. Metall. Eng.*, 2012, **1**, 130.

24. (a) J. Galy and G. Meunier, *J. Solid State Chem.*, 1975, **13**, 142; (b) P. A. Maggard, T. S. Nault, C. L. Stern and K. R. Poeppelmeier, *J. Solid State Chem.*, 2003, **175**, 25; (c) H. K. Izumi, J. E. Kirsch, C. L. Stern and K. R. Poeppelmeier, *Inorg. Chem.*, 2005, **44**, 884.

80 25. K. M. Ok and P. S. Halasyamani, *Inorg. Chem.*, 2005, **44**, 9353.